Dalton Transactions

ROYAL SOCIETY OF CHEMISTRY

PAPER

View Article Online
View Journal | View Issue

Check for updates

Cite this: *Dalton Trans.*, 2025, **54**, 17553

Magnesium catalyzed hydroamination of carbodiimides and hydroboration of cyanamides

Anubhab Das, Sayantan Mukhopadhyay, Sagrika Rajput and Sharanappa Nembenna *

Received 30th September 2025,
Accepted 27th October 2025

DOI: 10.1039/d5dt02335a

rsc.li/dalton

A β-diketiminate magnesium hydride complex, **Mg-1** [{LMgH}$_2$; L = ^{Dep}Nacnac = (DepNCMe)$_2$CH; Dep = 2,6-Et$_2$-C$_6$H$_3$], catalyzes the hydroamination of carbodiimides with primary aryl amines and the hydroboration of cyanamides with HBpin. The reactions proceed efficiently under mild conditions, affording a range of guanidines, *N*-borylformamidines, and *N*,*N*-bis-boryldiamines in high yields. Detailed stoichiometric experiments and the successful isolation of active catalysts/key intermediates, *i.e.*, magnesium anilide [{LMg-NH-C$_6$H$_4$-4-Me}$_2$] (**Mg-2**), magnesium amidinate [{LMg–N=CH–N(Et$_2$)}$_2$] (**Mg-3**), and magnesium guanidinate [LMg(N^{i}Pr)(N-*p*-tolyl)C-NH-^{i}Pr] (**Int-A2**) complexes, provided insights into the reaction mechanisms, enabling the elucidation of plausible catalytic cycles. These results highlight the potential of Earth-abundant magnesium-based catalysts for synthesizing valuable nitrogen-containing compounds.

Introduction

The catalytic functionalization of organic unsaturated substrates, particularly carbodiimides (CDI) and their isomers, cyanamides, is a cornerstone of modern organic synthesis, offering efficient routes to nitrogen-rich compounds. Representative products, including guanidines, *N*-silyl amines, and *N*-borylated amines, have diverse applications spanning pharmaceuticals, agrochemicals, organometallic chemistry, and materials science.[1] Among the numerous transformations involving these substrates, the hydroamination of CDIs and the hydroboration of cyanamides stand out due to their atom economy and their ability to deliver such valuable nitrogen-containing products.

The hydroamination of carbodiimides (RN=C=NR) yields guanidine derivatives (RN=C(NR′R″)NHR), which are fundamental intermediates, largely used in the chemical industries. Early studies demonstrated that primary aliphatic amines could react with carbodiimides without a catalyst under extreme conditions.[2] Similarly, cyclic secondary amines have been shown to react with carbodiimides under ambient conditions, affording tetra-substituted guanidines without the need for a catalyst.[3] However, primary aromatic and acyclic secondary amines, which possess significantly lower nucleophilicity, require catalytic activation.[4] Richeson and co-workers reported the first catalytic guanylation of primary aromatic amines with unactivated carbodiimides using a titanium amido complex in 2003.[5] Since then, significant efforts have been made to develop effective catalytic systems to carry out such reactions. Several transition-metal,[5,6] rare-earth element,[7] and main-group metal[1a–d,4,8] complexes have been extensively studied, focusing on improving the reaction efficiency and broadening the substrate scope.

Given the structural similarities between carbodiimides and their isomeric counterparts, cyanamides (R$_2$NC≡N), which feature a highly reactive nitrile group, they serve as ideal substrates for hydrofunctionalization reactions. Recently, hydroboration of cyanamides has been introduced as an efficient method to produce *N*-borylated compounds. These products, such as *N*-boryl formamidines and bis-borylated diamines, provide versatile synthons for downstream applications.[9] Although CDI hydrofunctionalization has been extensively explored,[6a,8a,10] the hydrofunctionalization of cyanamides is still in its very early stages. To date, there have been only two reports on the hydrofunctionalization of cyanamides in the literature.[11]

In recent years, the development of main-group metal-based catalytic systems has garnered increasing attention as less toxic, cost-effective alternatives to transition metal-based catalysts.[12] In particular, highly abundant, bio-compatible magnesium-based reagents and molecular complexes have been established as promising catalysts in hydroelementation of several unsaturated organic functionalities.[1a,8e,12b,13] In magnesium-catalyzed hydroboration, hydroamination, and hydrosilylation reactions, magnesium hydrides are often identified as the active catalytic species.[13a–e,14] However, to the best of our knowledge, magnesium hydride-catalyzed hydroamination of carbodiimides has not been reported to date.

School of Chemical Sciences, National Institute of Science Education and Research (NISER), Homi Bhabha National Institute (HBNI), Bhubaneswar, 752050, India. E-mail: snembenna@niser.ac.in

Thus, herein, we report ^{Dep}Nacnac stabilized magnesium hydride [{LMgH}$_2$; L = ^{Dep}Nacnac = (DepNCMe)$_2$CH; Dep = 2,6-Et$_2$-C$_6$H$_3$] (**Mg-1**) as an efficient catalyst for hydroamination of carbodiimides with primary aryl amines and selective hydroboration of cyanamides using pinacolborane (HBpin). These reactions proceed efficiently under mild conditions, yielding *N*,*N*′,*N*″-trisubstituted guanidines, *N*-borylated imines, and bis-borylated diamines in high yields. We have performed various stoichiometric experiments to isolate key intermediates involved in the catalytic cycle, and based on those outcomes, we have proposed plausible catalytic mechanisms.

Results and discussion

^{Dep}Nacnac stabilized magnesium hydride (**Mg-1**) [{LMgH}$_2$; L = ^{Dep}Nacnac = (DepNCMe)$_2$CH; Dep = 2,6-Et$_2$-C$_6$H$_3$], previously reported by Jones and co-workers,[15] was synthesized *via* a two-step process, *i.e.*, treatment of the free ^{Dep}Nacnac ligand with the commercially available di-*n*-butyl magnesium reagent, which affords a magnesium alkyl compound {LMg-^{n}Bu}$_2$. Subsequent addition of the phenylsilane into a solution of {LMg-^{n}Bu}$_2$ as a hydride source produces the desired magnesium hydride {LMgH}$_2$.[15]

Addition of primary amines to diisopropylcarbodiimide (DIC)

In this study, we have described catalytic hydroamination of carbodiimide with primary aryl amines. We began our investigation with *p*-toluidine (**2a**) and diisopropylcarbodiimide (**DIC**) as standard substrates. An initial study in the presence of 3 mol% of **Mg-1** under neat conditions at room temperature produced the corresponding product 1,3-diisopropyl-2-(*p*-tolyl) guanidine (**3a**) within 30 minutes, with a quantitative ^{1}H NMR conversion (Table S1 of the SI, entry 2). A decrease in catalyst loading from 3 to 1 mol% resulted in quantitative conversion within 3 h at ambient temperature, achieving the optimal reaction conditions (Table S1 of the SI, entry 4). The conversions were drastically reduced upon shortening the reaction time or reducing the catalyst load any further (Table S1 of the SI, entries 5–7). A reaction in C$_6$D$_6$ under the optimal conditions showed no difference in the conversion to **3a** (Table S1 of the SI, entry 8). As stated in the introduction, a catalyst-free reaction showed no conversion to **3a** even after 24 h at 80 °C (Table S1 of the SI, entry 1), justifying the requirement of a catalytic environment. With the optimized conditions in hand, we explored the substrate scope. Primary aryl amines with electron-donating (**2a** and **2b**) and electron-withdrawing substituents (**2c** and **2d**), as well as N-heterocyclic aryl amines (**2e** and **2f**), were treated with DIC in the presence of pre-catalyst **Mg-1** (Table 1). We observed complete conversion to the corresponding guanidine product within 3 h in every case. Interestingly, despite the limited solubility of 4-aminobenzonitrile (**2c**) in DIC, the reaction proceeded under neat conditions to yield the corresponding guanidine product, which is likely facilitated by localized dissolution between the solid amine and the liquid carbodiimide. The guanidine products (**3a–3f**) were confirmed by ^{1}H and ^{13}C{^{1}H} NMR spectroscopy (see the SI for NMR spectra). After successful hydroamination of DIC, we investigated the reaction with different carbodiimides, such as di-*tert*-butyl and di-*p*-tolyl carbodiimides; unfortunately, no product conversion was observed. This can be attributed to their increased steric bulk, which impedes the approach of the nucleophilic anilido species (**Mg-2**) toward the electrophilic carbon center of the carbodiimide. We also attempted **Mg-1** catalyzed hydroalkoxylation of carbodiimides with benzyl alcohol to synthesize *N*,*N*′-disubstituted isourea. However, the reaction was unsuccessful, yielding no detectable amount of the desired isourea product.

Table 1 Substrate scope for hydroamination of DIC with primary aryl amines[a,b]

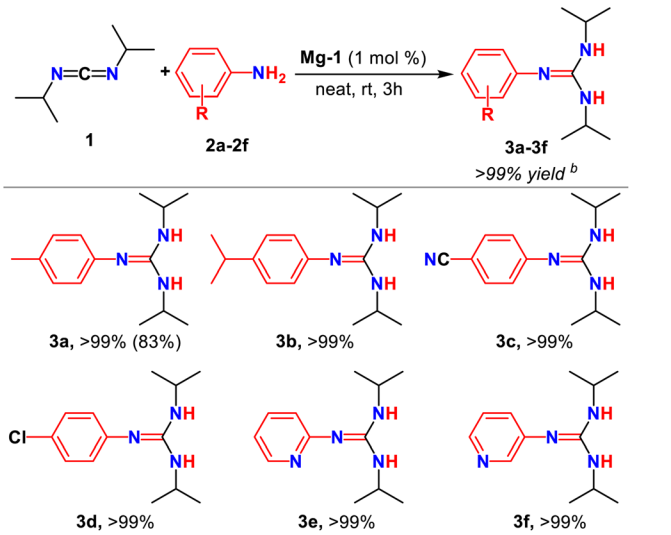

[a] Reaction conditions: DIC (**1**) (0.1 mmol, 1.0 equiv.), aryl amines **2a–2f** (0.1 mmol, 1.0 equiv.), pre-catalyst **Mg-1** (1 mol%), neat conditions, rt and 3 h. [b] Conversion was examined by ^{1}H and ^{13}C{^{1}H} NMR (400 MHz, 25 °C) spectroscopy based on the formation of the product and the consumption of the starting material. Isolated yield is shown in parentheses.

Hydroboration of cyanamides

Despite the advancement of metal-catalyzed hydrofunctionalization of unsaturated organic compounds, the hydroboration of cyanamides is rarely explored.[11] To overcome this limitation, we investigated the catalytic activity of **Mg-1** for this hydroboration. We used dibenzyl cyanamide (**4d**) as a model substrate, and HBpin as the hydroborating agent. An initial attempt at a catalyst-free reaction of **4d** with 1 equivalent of pinacolborane (HBpin) showed no conversion to the corresponding *N*-borylformamidine product (**5d**) after 24 h at 70 °C. The reaction with 3 mol% of the **Mg-1** catalyst at 70 °C under neat conditions afforded an incomplete conversion, yielding a mixture of unreacted cyanamide (**4d**), the *N*-borylformamidine product (**5d**), and the *N*,*N*-bis-boryldiamine product (**6d**), after 12 h (Table S2 of the SI, entry 2). Pleasingly, high selectivity was achieved by conducting the reaction in C$_6$D$_6$, which afforded

the desired product **5d** in quantitative yield (Table S2 of the SI, entry 3). The reaction produced quantitative conversion under reduced catalyst load of 1 mol% at 60 °C within 12 h, in C_6D_6, achieving the optimal reaction conditions (Table S2 of the SI, entry 5). Further decrease in catalyst loading to 0.5 mol% resulted in a decrease in yield even at a prolonged reaction time (Table S2 of the SI, entry 6).

With the optimized reaction conditions in hand, we expanded the substrate scope using aliphatic acyclic (**4a–4d**) and cyclic (**4e** and **4f**) cyanamides (Table 2). The ^{1}H NMR spectra show that dimethyl cyanamide yielded the corresponding *N*-borylformamidine product **5a** with a 67% NMR conversion, and furthermore, diethyl cyanamide showed complete conversion to **5b** with 1.5 equiv. of HBpin under the optimized conditions. Bulkier substituted cyanamide (**4c**) showed full conversion under the optimized reaction conditions. Cyclic cyanamides were also reduced to their corresponding *N*-borylformamidine products (**5e** and **5f**), yielding up to 92% in 12 h at 60 °C. Longer heating of the same resulted in the formation of trace amounts of dihydroborated products. The *N*-borylformamidine products (**5a–5f**) were confirmed by ^{1}H and ^{13}C{^{1}H} NMR spectroscopy. The ^{1}H NMR spectra revealed a new singlet peak in the 7.99–8.46 ppm region corresponding to the NC*H*N proton (see the SI for NMR spectra).

After successful monohydroboration of cyanamides, we aimed to fully reduce the cyanamides. A reaction of 2.1 equivalents of HBpin with **4d** in the presence of 5 mol% of **Mg-1** yielded the corresponding *N*,*N*-bis-boryldiamine product (**6d**) after 18 h at 80 °C under neat conditions (Table S3 of the SI, entry 2). A reduction in the catalyst loading to 2 mol% produced complete NMR conversion to **6d** after 18 h at 70 °C (Table S3 of the SI, entry 4), achieving the optimal conditions. Further decreasing the catalyst loading significantly decreased product conversion, resulting in the mixture **6d** and the *N*-borylformamidine **5d** (Table S3 of the SI, entries 5 and 6).

With the optimized reaction conditions in hand, we explored the substrate scope using cyanamides **4b–4f** (Table 3). The *N*,*N*-bis-boryldiamine products (**6b–6f**) were confirmed by ^{1}H and ^{13}C{^{1}H} NMR spectroscopy. The ^{1}H NMR spectra show a new singlet peak in the 3.88–4.37 ppm region corresponding to NCH_2N protons (see the SI for NMR spectra). The cyanamides **4c–4f** showed full conversion to their corresponding *N*,*N*-bis-borylated products under the optimized conditions. However, for dimethyl (**4a**) and diethyl (**4b**) cyanamides, we observed a mixture of mono and dihydroborated products under the optimized conditions. The monohydroboration of cyanamides proceeded smoothly in C_6D_6, whereas under neat conditions, a mixture of mono- and dihydroborated products was obtained, highlighting a distinct solvent effect of C_6D_6 in directing the selectivity of the reaction as the concentration of reactants is lower in the solution compared to neat conditions. However, the complete hydroboration to the dihydroborated product proceeded efficiently under neat conditions, although the reaction of diethyl cyanamide (**4b**) required 3 equiv. of HBpin in C_6D_6 in the presence of 2 mol% of **Mg-1** to afford the corresponding product **6b** with a >99% NMR conversion after 18 h at 70 °C. After achieving selective hydroboration of cyanamides under mild reaction conditions, we further investigated hydrosilylation of cyanamides. However, attempts at the **Mg-1** catalyzed hydrosilylation of these substrates were unsuccessful.

Table 2 Substrate scope for monohydroboration of cyanamides[a,b,c]

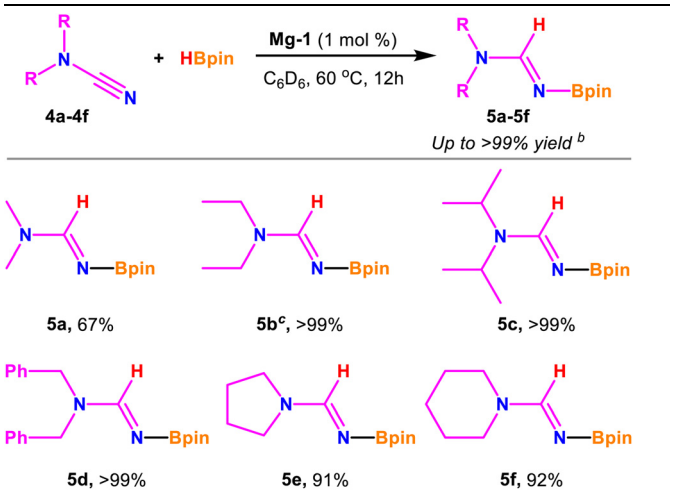

[a] Reaction conditions: cyanamides (**4a–4f**) (0.2 mmol, 1.0 equiv.), HBpin (0.2 mmol, 1.0 equiv.), catalyst **Mg-1** (1 mol%), C_6D_6, 60 °C and 12 h. Conversion was examined by ^{1}H NMR spectroscopy based on the appearance of the new characteristic proton resonance (NC*H*N) of the product. [b] Yields were calculated using mesitylene as an internal standard (0.2 mmol, 1.0 equiv.). [c] 1.5 equiv. HBpin was used.

Table 3 Substrate scope for dihydroboration of cyanamides[a,b,c]

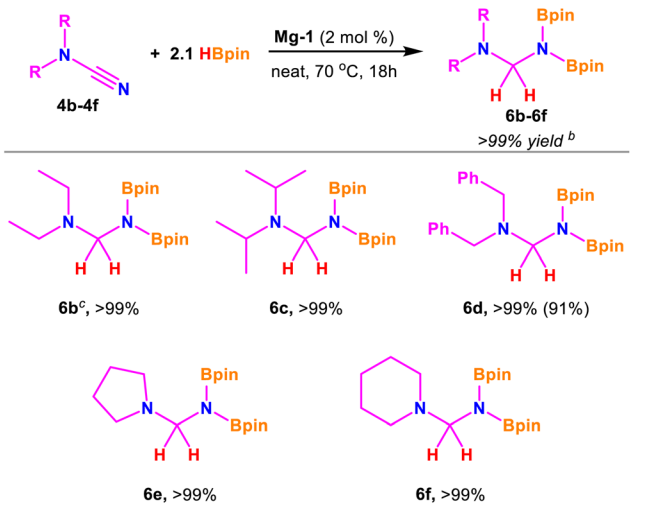

[a] Reaction conditions: cyanamides (**4b–4f**) (0.1 mmol, 1.0 equiv.), HBpin (0.21 mmol, 2.1 equiv.), catalyst **Mg-1** (2 mol%), neat conditions, 70 °C and 18 h. [b] Conversion was examined by ^{1}H NMR spectroscopy based on the appearance of the new NCH_2N(Bpin)$_2$ resonance of the products. [c] Reaction was performed in C_6D_6 in a J. Young valve NMR tube at 70 °C for 18 h, 3.0 equiv. HBpin. Isolated yield is shown in parentheses.

Scale-up reactions

To explore the practical application of the magnesium hydride complex (**Mg-1**), we performed a large-scale reaction of carbodiimide with *p*-toluidine (**2a**) under the optimized conditions. A 5 mmol scale reaction of DIC (**1**) with 1 equiv. of *p*-toluidine (**2a**) yielded the product 1,3-diisopropyl-2-(*p*-tolyl) guanidine (**3a**) in 83% yield (Scheme 1a).

For the dihydroboration of cyanamides, a 2 mmol scale reaction was performed with dibenzyl cyanamide (**4d**) and 2.1 equiv. of HBpin (Scheme 1b). Under the standard reaction conditions, it produced the corresponding *N*,*N*-bis-boryldiamine product (**6d**) in an isolated yield of 91%.

Attempts to scale up the monohydroboration of cyanamides under the optimized conditions resulted in the formation of a mixture containing the desired monohydroborated product along with a minor amount of the dihydroborated species; hence, further scale-up was not pursued.

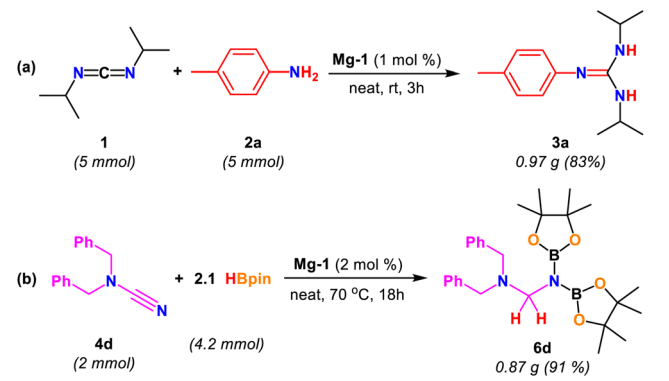

Scheme 1 Scale-up reactions.

Stoichiometric experiments

Hydroamination of carbodiimides. To gain insight into the reaction mechanism, we performed several control experiments. A 1 : 2 stoichiometric reaction between **Mg-1** and *p*-toluidine (**2a**) in C_6D_6 resulted in the formation of a magnesium anilide complex **Mg-2** [{LMg-NH-C_6H_4-4-Me}$_2$] immediately at room temperature (Scheme 2a). **Mg-2** was characterized by ^{1}H and ^{13}C{^{1}H} NMR spectroscopy and single-crystal X-ray diffraction studies. The ^{1}H NMR spectrum shows a complete disappearance of the Mg–*H* signal at 3.85 ppm and the appearance of a new peak at 6.03 ppm corresponding to the N*H* proton of the anilide moiety. Notably, the γ-C*H* resonance of the NCCCN backbone of **Mg-1** (δ 4.79 ppm in C_6D_6) shows a slightly upfield shift to δ 4.73 ppm, indicating the formation of **Mg-2**.

Single crystals suitable for X-ray diffraction studies were grown in a vial through slow evaporation of C_6D_6. X-ray diffraction analysis showed that **Mg-2** crystallizes in a triclinic system with a $P\bar{1}$ space group. The solid-state structure (Fig. 1) exhibits a dimeric structure, in which the magnesium center adopts a distorted tetrahedral geometry, bonded to one Nacnac ligand in an *N*,*N*′-chelated fashion, and the other two sites are occupied by N atoms of the anilide moieties. The Mg1–N3 bond distance in **Mg-2** is 2.0802(13) Å, which is slightly shorter than the previously reported Mg–N bond distance of a ^{Dipp}Nacnac magnesium anilide complex (2.1251(16) Å).[16] The N1–Mg1–N2 bite angle is 94.32(5)°, which is slightly wider than the reported bite angle (92.65(6)°).[16] Moreover, **Mg-2** was tested as a catalyst for the hydroamination reaction between DIC (**1**) and *p*-toluidine (**2a**), affording the desired guanidine product (**3a**) in quantitative yield (Table S1, entry 9).

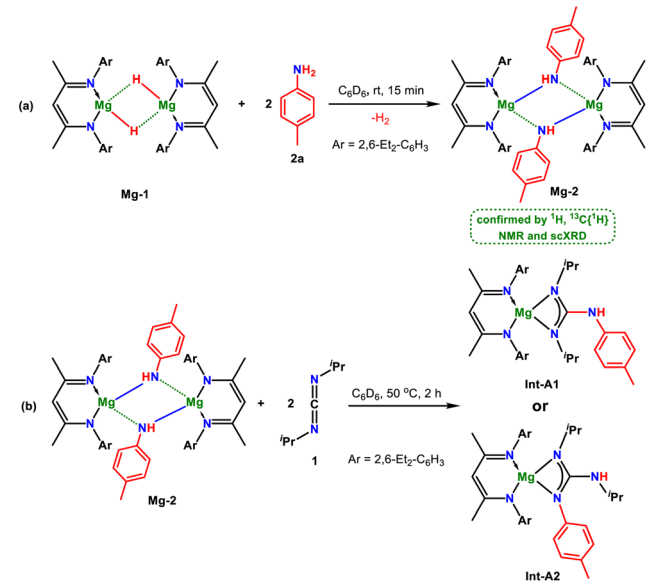

Scheme 2 Stoichiometric experiments.

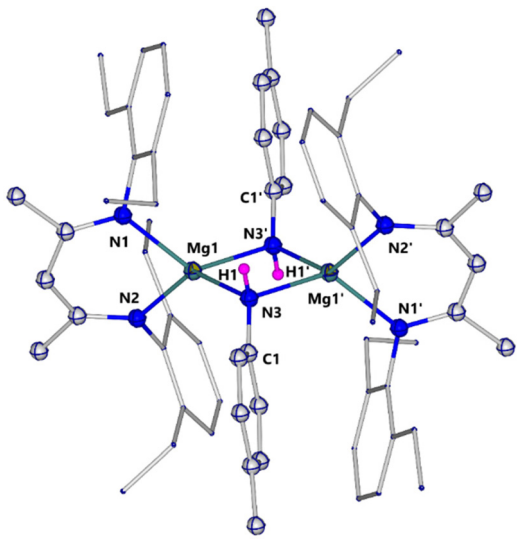

Fig. 1 Solid-state structure of **Mg-2**. Hydrogen atoms except H1 were omitted for better visibility. The selected bond distances (Å) and bond angles (°) are: Mg1–N1 2.0465(13), Mg1–N2 2.0358(13), Mg1–N3 2.0802 (13), N3–C1 1.4178(19), N1–Mg1–N2 94.32(5), N1–Mg1–N3 108.17(5), N2–Mg1–N3 129.39(6), and Mg1–N3–Mg1′ 91.00(5).

Furthermore, the addition of 2.0 equiv. of DIC (**1**) to **Mg-2** in C_6D_6 at 50 °C for 2 h afforded the magnesium guanidinate complex **Int-A2** [LMg(N^{i}Pr)(N-*p*-tolyl)-C-NH-^{i}Pr] (Scheme 2b). In the ^{1}H NMR spectrum of **Int-A2**, the γ-C*H* resonance exhibits a downfield shift to 4.93 ppm (δ 4.73 ppm in **Mg-2**). The isopropyl methyl protons resonate as two distinct doublets at 0.65 and 0.62 ppm. Meanwhile, the N*H* signal of **Int-A2** appears at 3.22 ppm as a doublet signal, markedly shifted from 6.03 ppm in **Mg-2**. Furthermore, the peak at 164.4 ppm in the $^{13}C\{^1H\}$ NMR spectrum corresponding to the NC*N* carbon confirms the formation of **Int-A2**. Moreover, the possibility of the formation of another intermediate, **Int-A1**, has been ruled out by the distinct doublet signal for the N*H* proton at 3.22 ppm in the ^{1}H NMR spectrum, together with previously reported literature on aluminum-catalyzed hydroamination of carbodiimides, suggesting that **Int-A2** is more favourable.[4] Additionally, **Int-A2** has been confirmed by mass spectrometry. Literature surveys show that the metal-catalyzed synthesis of guanidines from carbodiimide and primary amines involves two steps: first, the formation of a metal anilide complex, and second, the insertion of carbodiimide into the metal–nitrogen bond.[1a–d,4,6,17] The isolation of **Mg-2** and **Int-A2** confirms that the hydroamination of carbodiimides follows the same pathway.

From the catalytic reaction and stoichiometric experiments, a notable difference in reaction conditions was observed. In the stoichiometric reaction, external heating was necessary to facilitate the formation of **Int-A2**. In contrast, during catalysis, the *in situ* generation of **Mg-2** was accompanied by exothermic H_2 evolution, which provided sufficient thermal energy to promote the insertion step even at room temperature. This phenomenon became particularly evident during the scale-up experiment, where noticeable heating of the reaction flask was observed.

Hydroboration of cyanamides. A 1 : 2 ratio stoichiometric reaction was conducted with **Mg-1** and diethyl cyanamide (**4b**) in C_6D_6 (Scheme 3a). This afforded the magnesium amidinate complex **Mg-3** [{LMg–N=CH–N(Et$_2$)}$_2$] after 15 minutes at room temperature. **Mg-3** was characterized by ^{1}H and $^{13}C\{^1H\}$ NMR spectroscopy and X-ray diffraction analyses. In the ^{1}H NMR spectrum, the Mg–H resonance at 3.85 ppm disappeared, and concurrently a new singlet at 7.59 ppm appeared, corresponding to the NC*H*N moiety. Moreover, the $^{13}C\{^1H\}$ NMR spectrum shows a peak at 152.8 ppm corresponding to the N*C*HN carbon, confirming the insertion of the Mg–H bond into the N–C≡N moiety of the cyanamide. Single crystals suitable for X-ray diffraction analyses were grown in C_6D_6 in the J. Young valve NMR tube. The X-ray diffraction analyses show that **Mg-3** crystallizes in a monoclinic system with a $P2_1/n$ space group. The molecular structure unfolds a dimeric unit, in which the magnesium center adopts a distorted tetrahedral geometry, bonded to the Nacnac ligand at two sites and the other two sites with N atoms of the amidinate moiety (Fig. 2). The N3–C1 bond length (*i.e.*, 1.267(2) Å) closely resembles the N=C double bond lengths (1.263(2) Å for ^{Dipp}NacnacMg-N=CH-C$_6$H$_4$-3-OMe and 1.271(2) Å for ^{Dipp}NacnacMg-N=CH-C$_6$H$_4$-4-OMe) reported in the literature.[13c]

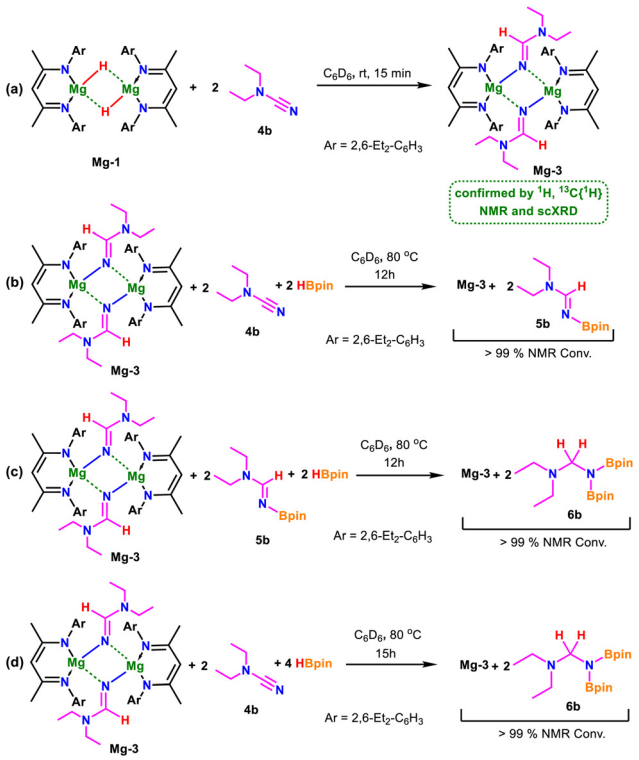

Scheme 3 Stoichiometric experiments.

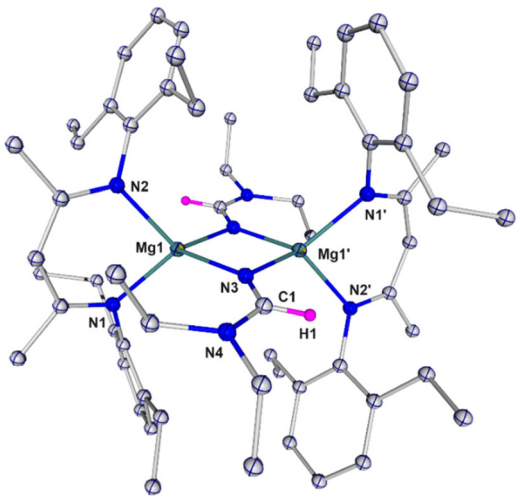

Fig. 2 Solid-state structure of **Mg-3**. Thermal ellipsoids are shown at 50% probability. Hydrogen atoms except H1 were omitted for better visibility. The selected bond distances (Å) and bond angles (°) are: Mg1–Mg1′ 2.9000(9), Mg1–N1 2.0740(13), Mg1–N2 2.0598(13), Mg1–N3 2.0462(13), N3–C1 1.267(2), C1–N4 1.371(2), N1–Mg1–N2 90.69(5), N1–Mg1–N3 119.43(5), N2–Mg1–N3 120.69(5) and Mg1–N3–C1 146.14(11).

Further reaction of **Mg-3** with 2 equiv. of HBpin showed no conversion, with the reactants remaining intact even after 24 h at 80 °C. Addition of 2 equiv. of diethyl cyanamide (**4b**) to the reaction mixture yielded the monohydroboration product **5b** (Scheme 3b) with the regeneration of **Mg-3** after 12 h at 80 °C.

The ^{1}H NMR spectrum exhibited two downfield singlets, confirming the presence of both **5b** and **Mg-3** (Fig. S7 of the SI). The resonance at 8.12 ppm corresponds to the NC*H*N proton of **5b** and the signal at 7.59 ppm corresponds to the Mg–NC*H*N(Et)$_2$ proton of **Mg-3**. Subsequent addition of another 2.0 equiv. of HBpin to the same reaction mixture led to quantitative conversion into a dihydroboration product, **6b**, along with **Mg-3** under the same reaction conditions (Scheme 3c). The signal at 7.59 ppm in the ^{1}H NMR spectrum (Fig. S8 of the SI) corresponds to the Mg–NC*H*N(Et)$_2$ of **Mg-3**, and the signal at 4.41 ppm indicates the NCH_2N protons of **6b**. Notably, the direct reaction of **Mg-3** with 2.0 equiv. of **4b** and 4 equiv. of HBpin afforded **6b**, accompanied by regeneration of **Mg-3** (Scheme 3d). The aforementioned results indicate that magnesium hydride **Mg-1** is the pre-catalyst, which forms **Mg-3** and then continues the catalytic cycle as the active catalyst.

Recently, Thomas and co-workers demonstrated that BH_3 generated from the decomposition of HBpin can serve as a hidden catalyst for the hydroboration reactions.[18] To rule out this possibility, a reaction of excess HBpin with the catalyst **Mg-1** was conducted; however, we did not observe the formation of BH_3 in ^{11}B NMR spectroscopy (Fig. S9 of the SI). Moreover, a catalytic reaction was carried out in the presence of *N*,*N*,*N*′,*N*′-tetramethylethylenediamine (TMEDA) under the optimized conditions; however, no noticeable decrease in conversion was observed in the ^{1}H NMR spectrum (Fig. S10 of the SI). The aforementioned result and isolation of **Mg-3** indicate that **Mg-1** is the primary catalyst, and no hidden boron catalysis is involved in the reactions.

The catalytic hydroboration of **4d** was monitored *via in situ* studies by reacting with 2.1 equiv. of HBpin in the presence of 2 mol% of **Mg-1**, with the reaction progress being tracked at variable temperatures over different time intervals. Time-stacked variable temperature NMR spectra revealed the stepwise formation of *N*-borylformamidine (**5d**) and *N*,*N*-bis-boryldiamine (**6d**) products. Initially, we observed a singlet signal at 8.46 ppm corresponding to the NC*H*N proton, confirming the formation of **5d**. Upon increasing the temperature to 70 °C, a new signal appeared at 4.06 ppm corresponding to the NCH_2N proton of **6d**, and the signal at 8.46 ppm disappeared, indicating the complete consumption of **5d** (Fig. 3).

As mentioned earlier, we attempted **Mg-1** catalyzed O–H bond addition to DIC, which was unsuccessful. However, a 1 : 2 ratio stoichiometric reaction between **Mg-1** and benzyl alcohol in C_6D_6 yielded the magnesium alkoxide complex **Mg-4** [{LMg–O–CH_2–C_6H_5}$_2$, L = ^{Dep}Nacnac = (DepNCMe)$_2$CH; Dep = 2,6-Et$_2$-C_6H_3] (Scheme 4). **Mg-4** was confirmed by both ^{1}H and ^{13}C{^{1}H} NMR spectroscopy. ^{1}H NMR analysis shows a singlet at 4.92 ppm signaling the γ-C*H* proton, downfield shifted compared to **Mg-1** (4.79 ppm in C_6D_6). The sharp singlet at 4.50 ppm, corresponding to the OCH_2 protons, further confirmed the formation of **Mg-4**. Single crystals suitable for X-ray diffraction analysis were obtained inside the NMR tube. The X-ray diffraction data show that **Mg-4** crystallizes in a monoclinic system with a $P2_1/n$ space group (Fig. 4). It exhibits a dimeric unit bridged by the oxygen atom (Mg–O–Mg). The magnesium center adopts a distorted tetrahedral geometry, bonded to one Nacnac ligand in an *N*,*N*′-chelated fashion, and the other two sites by O atoms. The Mg–O bond distance, *i.e.*, 1.9535(15) Å, is shorter in comparison with the ^{Dipp}Nacnac analogue (1.998(6) Å).[19] The N–Mg–N bite angle is 92.42(7)°, which is in good agreement with the previously reported bite angle, *i.e.*, 92.2(2)°.[19]

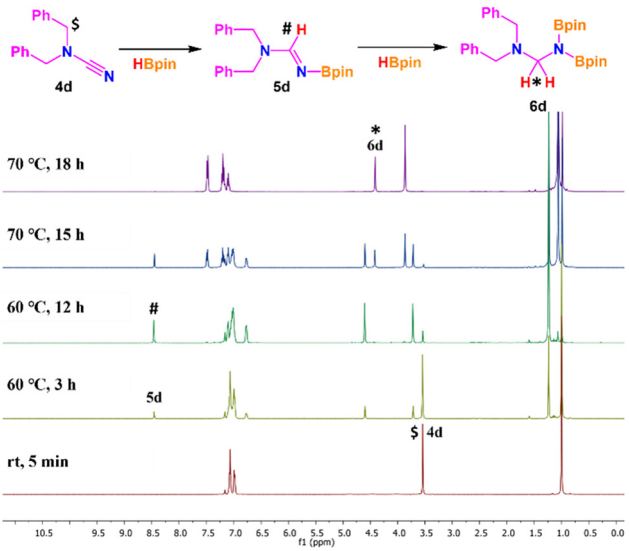

Fig. 3 Stacked ^{1}H NMR spectra (400 MHz) for the reaction of **4d** (0.1 mmol, 1.0 equiv.), HBpin (0.21 mmol, 2.1 equiv.) and **Mg-1** (2 mol%) in C_6D_6. Spectra recorded at different temperatures and time intervals (*T* = 25–70 °C and *t* = 5 min to 18 h).

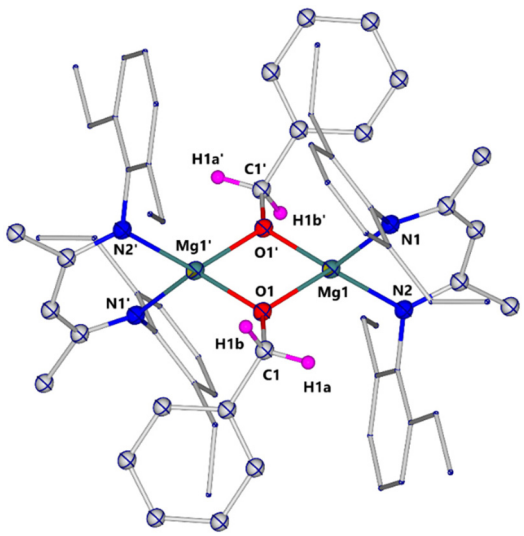

Fig. 4 Solid-state structure of **Mg-4**. Hydrogen atoms except H1a and H1b were omitted for better visibility. The selected bond distances (Å) and bond angles (°) are: Mg1–N1 2.0403(18), Mg1–N2 2.0595(17), Mg1–O1 1.9535(15), O1–C1 1.406(3), N1–Mg1–N2 92.42(7), O1–Mg1–O1′ 83.86(6), N1–Mg1–O1′ 124.28(7), and N2–Mg1–O1 127.00(7).

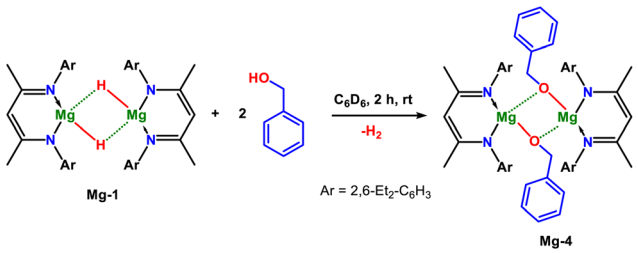

Scheme 4 Synthesis of compound **Mg-4**.

Catalytic cycles

Hydroamination of carbodiimides. Based on the results of the above stoichiometric experiments and previously documented mechanisms in the literature,[1d,7b,f] we proposed a plausible catalytic cycle for N–H bond addition to CDIs as shown in Scheme 5.

In this reaction, **Mg-1** acts as a pre-catalyst, which reacts with the primary aryl amine to form the magnesium anilide (**Mg-2**) complex with the release of H_2 gas. A subsequent addition of the carbodiimide to the magnesium anilide complex forms the guanidinate intermediate, **Int-A2**. Furthermore, intermediate **Int A2** independently reacts with an aryl amine, affords the corresponding guanidine product, and closes the cycle with the regeneration of the active catalyst **Mg-2**.

Hydroboration of cyanamides. Based on the stoichiometric reactions, we proposed a catalytic cycle for the hydroboration of cyanamides, as represented in Scheme 6. In this reaction, magnesium hydride **Mg-1** acts as a pre-catalyst, contrary to the reported mechanism where metal (zinc) hydride acts as the active catalyst.[11a] In the zinc system, the bis-guanidinate zinc hydride itself participates directly as the active species in B–H bond addition and regenerates at the end of the catalytic cycle, while in this case, **Mg-1** first reacts with cyanamide **4b** to generate the magnesium amidinate complex **Mg-3**, which functions as the active catalyst. HBpin reacts with **Mg-3** to form the borohydride intermediate **Int-B**, consistent with the type of borohydride species previously described in magnesium-catalyzed hydroboration reactions.[13a–d] **Int-B** further reacts with diethyl cyanamide (**4b**) to regenerate the active catalyst **Mg-3** with the formation of monohydroboration products **5b**.

For the dihydroboration reaction, **Int-B** reacts with cyanamide **4b** and another equivalent of HBpin to form the dihydroboration product **6b** and completes the cycle with the regeneration of **Mg-3**.

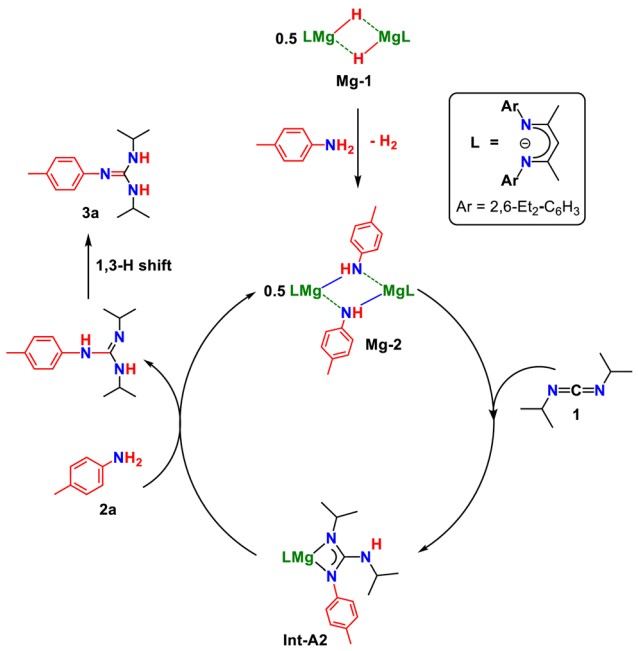

Scheme 5 Proposed catalytic cycle for hydroamination of DIC.

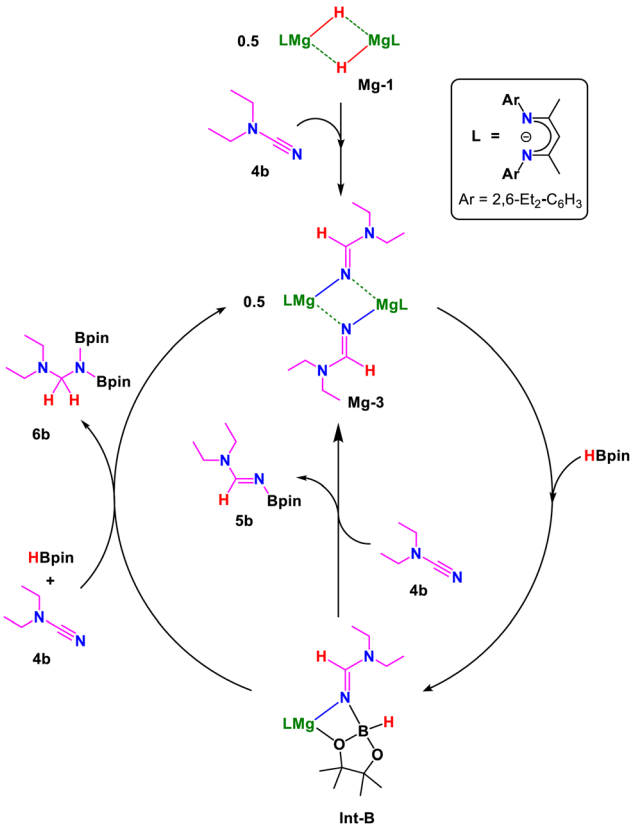

Scheme 6 Proposed catalytic cycle for hydroboration of cyanamides.

Conclusions

In conclusion, we have demonstrated a method for hydroamination of CDI and chemoselective hydroboration of cyanamides using a β-diketiminate magnesium hydride (pre-)catalyst under mild conditions. The method accommodates the synthesis of a range of guanidine, *N*-borylformamidine, and *N*,*N*-bis-boryldiamine products with high chemoselectivity and yields. Compared with previously reported magnesium-based

catalysts for similar hydroamination reactions,[1a,8e,13f] the present system exhibits enhanced efficiency, achieving comparable or superior conversions under milder conditions, including lower catalyst loadings, under solvent-free conditions, and even at ambient temperature. Notably, in cyanamide hydroboration, **Mg-1** achieved complete conversions under comparatively lower catalyst loadings than that of the recently developed zinc-based system.[11a] However, we noticed that the catalytic activity of **Mg-1** is comparable to that of a recently reported bis(guanidinate) magnesium catalyst.[11b] Moreover, the solvent was found to play a decisive role in controlling the product selectivity, with C_6D_6 favoring monohydroboration while neat conditions promoted full reduction to *N*,*N*-bis-boryldiamines. Additionally, we have isolated active catalysts and key intermediates involved in the reaction mechanism, namely magnesium anilide complex (**Mg-2**) and magnesium amidinate complex (**Mg-3**), which were characterized by multinuclear NMR spectroscopy and single-crystal X-ray diffraction analyses. Furthermore, plausible catalytic cycles have been proposed based on the isolation of key intermediates and stoichiometric experiments.

Experimental section

Methods

Unless stated, all the reactions were performed under an inert nitrogen atmosphere using standard Schlenk and glovebox techniques. Silicone-greased glassware and vessels with J. Young valves were used. NMR spectroscopic data were recorded on a Bruker AV 400 MHz or 700 MHz Bruker DPX spectrometer [$^{13}C\{^1H\}$, 101 MHz or 176 MHz]. Deuterated benzene (C_6D_6) and chloroform ($CDCl_3$) were used for NMR measurements; chemical shift values (δ) were reported in parts per million relative to the residual signals of their respective solvents.[20] Coupling constants (J) are given in Hz. The multiplicity of the ^1H NMR spectrum is given as follows: s = singlet, d = doublet, t = triplet, q = quartet, dd = doublet of doublets, dt = doublet of triplets, br = broad, and m = multiplet signal. Mass spectrometry analyses were performed on a Waters XevoG2 XS Q-TOF mass spectrometer. The single crystals of compounds **Mg-2**, **Mg-3**, and **Mg-4** were grown in vials from C_6D_6 inside the glove box at rt. The single crystal data were collected on a Rigaku Oxford diffractometer with graphite-monochromated Cu-Kα radiation (λ = 1.54184 Å) at 100 K. Selected data collection parameters and other crystallographic results are summarized in Table S4 of the SI.

Materials

All the solvents were purified by distillation over Na/benzophenone and stored in a dinitrogen atmosphere with activated molecular sieves. Deuterated chloroform ($CDCl_3$) was dried with molecular sieves, and deuterated benzene (C_6D_6) was dried over a Na mirror, distilled, and degassed. The β-diketimine ligand was prepared according to the reported literature procedures. For catalytic reactions, J. Young valve NMR tubes were thoroughly dried in an oven before use. All the chemicals and the reagents were supplied by Sigma-Aldrich Co. Ltd, TCI Chemicals, and Merck India Pvt. Ltd and were utilized without any further purification. The catalyst [^{Dep}**NacnacMg(μ-H)]$_2$** (**Mg-1**) was prepared according to the reported literature.[15]

General procedure for hydroamination of DIC

DIC (0.1 mmol, 1 equiv.), aryl amines (0.1 mmol, 1.0 equiv.) and 0.001 mmol (1 mol%) of catalyst **Mg-1** were charged in a vial with a magnetic bead inside a glove box. The vial was closed and stirred at room temperature for 3 h. The progress of the reaction was monitored using ^1H NMR spectroscopy.

General procedure for catalytic monohydroboration of cyanamides

Cyanamides (0.2 mmol, 1 equiv.) and 0.002 mmol (1 mol%) of catalyst **Mg-1** were charged in a J. Young valve NMR tube inside a glove box. Then, C_6D_6 (~0.5 mL) was added, followed by HBpin (0.2 mmol, 1 equiv.). The NMR tube was removed from the glove box and heated at 60 °C for 12 h. The progress of the reaction was monitored using ^1H NMR spectroscopy, which indicated the completion of the reaction by observing the characteristic NC*H*N(Bpin) peak.

General procedure for catalytic dihydroboration of cyanamides

Cyanamides (0.1 mmol, 1 equiv.), HBpin (0.21 mmol, 2.1 equiv.) and 0.002 mmol (2 mol%) of catalyst **Mg-1** were charged in a vial with a magnetic bead or in a J. Young valve NMR tube inside a glove box. The sealed vial or NMR tube was removed from the glove box and heated/stirred at 70 °C for 18 h. The progress of the reaction was monitored using ^1H NMR spectroscopy, which indicated the completion of the reaction by observing a characteristic NCH_2N(Bpin)$_2$ peak.

Synthesis of Mg-2, Int-A2, Mg-3 and Mg-4

Synthesis of [LMgNH-C_6H_4-4-Me]$_2$ (Mg-2) {NMR scale}. Addition of 5.6 mg of *p*-toluidine (0.052 mmol, 2 equiv.) to a solution of **Mg-1** (20 mg, 0.026 mmol, 1.0 equiv.) in C_6D_6 (~0.5 mL) in a J. Young valve NMR tube yielded the magnesium anilide complex (**Mg-2**) within 15 min at room temperature. Single crystals suitable for X-ray diffraction were grown in a vial inside the glovebox at room temperature. NMR conversion >99%. ^1H NMR (400 MHz, C_6D_6, 298 K) δ = 7.18 (dd, J = 13.9, 6.1 Hz, 8H, Ar–*H*), 7.10 (d, J = 23.1 Hz, 8H, Ar–*H*), 6.73 (d, J = 7.4 Hz, 4H, Ar–*H*), 6.03 (d, J = 5.0 Hz, 2H, N*H*), 4.73 (s, 2H, C*H*), 2.52 (bs, 4H, CH_2CH$_3$), 2.24 (bs, 6H, CH_2CH$_3$), 2.18 (s, 6H, *p*-CH_3), 1.79 (bs, 6H, CH_2CH$_3$), 1.48 (s, 12H, CCH_3), 1.05 (m, 24H, CH$_2$CH_3). $^{13}C\{^1H\}$ NMR (101 MHz, C_6D_6, 298 K) δ = 168.5, 150.4, 147.6, 137.8, 137.2, 129.7, 126.1, 124.7, 120.6, 95.2, 24.3, 23.7, 20.7, 13.6. Due to the highly air and moisture-sensitive nature of the complex, we were unable to produce HRMS data for the appropriate intensity ratio or an adequate percentage in the elemental analysis report.

Synthesis of [LMg(N^{i}Pr)(N-*p*-tolyl)-C-NH-^{i}Pr] (Int-A2) {NMR scale}. To the NMR tube containing a solution of **Mg-2** (0.26 mmol, 1.0 equiv.) in C_6D_6, DIC (8 μL, 0.52 mmol, 2.0 equiv.) was added and heated at 50 °C for 2 h. It afforded us the

magnesium guanidinate complex **Int-A2**. NMR conversion >99%. ^{1}H NMR (400 MHz, C_6D_6, 298 K) δ = 7.11 (dd, J = 9.3, 4.0 Hz, 6H, Ar–*H*), 6.98 (d, J = 8.1 Hz, 2H, Ar–*H*), 6.81 (d, J = 8.2 Hz, 2H, Ar–*H*), 4.93 (s, 1H, C*H*), 3.45–3.33 (m, 2H, ^{i}Pr–C*H*), 3.22 (d, J = 9.8 Hz, 1H, N*H*), 2.79–2.65 (m, 8H, CH_2CH_3), 2.23 (s, 3H, *p*-CH_3), 1.68 (s, 6H, CCH_3), 1.21 (t, J = 7.3 Hz, 12H, CH_2CH_3), 0.65 (d, J = 6.2 Hz, 6H, ^{i}Pr-CH_3), 0.62 (d, J = 6.3 Hz, 6H, ^{i}Pr-CH_3). $^{13}C\{^1H\}$ NMR (101 MHz, C_6D_6, 298 K) δ = 168.8, 164.4, 148.5, 147.1, 137.2, 129.6, 127.5, 125.5, 124.7, 122.0, 94.9, 44.3, 44.3, 24.8, 24.7, 23.3, 23.0, 20.9, 13.7. HRMS (ASAP/Q-TOF) m/z: $[M + H]^+$ calcd for $C_{39}H_{56}MgN_5$ 618.4386, Found: 618.4354.

Synthesis of [LMgNC(H)N(Et$_2$)]$_2$ (Mg-3) {NMR scale}. Addition of 5.9 μL of diethyl cyanamide (0.052 mmol, 2 equiv.) to a J. Young valve NMR tube containing a solution of compound **Mg-1** (20 mg, 0.026 mmol, 1.0 equiv.) in dry C_6D_6 (~0.5 mL) resulted in the formation of the magnesium amidinate complex **Mg-3** within 15 minutes at room temperature. Then, the contents of the NMR tube were transferred to a vial inside the glove box to grow single crystals suitable for X-ray diffraction. NMR conversion >99%. ^{1}H NMR (400 MHz, C_6D_6, 298 K) δ = 7.59 (s, 2H, NC*H*N), 7.14 (s, 4H, Ar–*H*), 7.12 (s, 2H, Ar–*H*), 7.10 (s, 4H, Ar–*H*), 7.08 (d, J = 2.3 Hz, 4H, Ar–*H*), 4.78 (s, 2H, C*H*), 3.12 (broad s, 4H, CH_2CH_3), 2.99 (broad s, 4H, CH_2CH_3), 2.49 (dq, J = 15.1, 7.5 Hz, 8H, CH_2CH_3), 2.10 (broad dd, J = 14.0, 6.1 Hz, 8H, CH_2CH_3), 1.50 (s, 12H, CCH_3), 1.12 (t, J = 7.6 Hz, 24H, CH_2CH_3), 0.90 (broad s, 12H, CH_2CH_3). $^{13}C\{^1H\}$ NMR (176 MHz, C_6D_6, 298 K) δ = 167.5, 152.8, 148.4, 137.3, 125.8, 123.9, 94.6, 45.7, 23.7, 23.7, 14.3, 12.7. Due to the highly air and moisture-sensitive nature of the complex, we were unable to produce HRMS data for the appropriate intensity ratio or an adequate percentage in the elemental analysis report.

Synthesis of [LMg-O-CH$_2$-C$_6$H$_5$]$_2$ (Mg-4) {NMR scale}. 5.4 μL of benzyl alcohol (0.052 mmol, 2.0 equiv.) was added to a J. Young valve NMR tube containing a solution of **Mg-1** (20 mg, 0.026 mmol, 1 equiv.) in C_6D_6 (~0.5 mL) inside a glovebox. This resulted in the formation of the magnesium alkoxide complex **Mg-4** after 2 h at room temperature. Within 48 h, we obtained block-shaped single crystals suitable for X-ray diffraction analysis inside the NMR tube. NMR conversion = 99%. ^{1}H NMR (400 MHz, C_6D_6, 298 K) δ = 7.22 (t, J = 7.5 Hz, 4H, Ar–*H*), 7.19 (s, 6H, Ar–*H*), 7.11 (d, J = 7.3 Hz, 8H, Ar–*H*), 7.07–7.01 (m, 4H, Ar–*H*), 4.92 (s, 2H, C*H*), 4.50 (s, 4H, OCH_2), 2.34 (dd, J = 15.3, 7.6 Hz, 8H, CH_2CH_3), 2.06 (dd, J = 15.3, 7.6 Hz, 8H, CH_2CH_3), 1.47 (s, 12H, CCH_3), 1.04 (t, J = 7.5 Hz, 24H, CH_2CH_3). $^{13}C\{^1H\}$ NMR (101 MHz, C_6D_6, 298 K) δ = 168.7, 147.7, 144.9, 137.5, 128.9, 127.4, 126.7, 126.0, 124.5, 95.7, 66.4, 23.8, 23.8, 14.2. Due to the highly air and moisture-sensitive nature of the complex, we were unable to produce HRMS data for the appropriate intensity ratio or an adequate percentage in the elemental analysis report.

Author contributions

The manuscript was written with contributions from all authors. All authors have approved the final version of the manuscript.

Conflicts of interest

There are no conflicts to declare.

Data availability

The data supporting this article have been included as part of the supplementary information (SI). Supplementary information: ^{1}H and $^{13}C\{^1H\}$ NMR spectra of compounds **Mg-2**, **Mg-3**, **Mg-4**, and **Int-A2**, stoichiometric experiments, and catalytic products. See DOI: https://doi.org/10.1039/d5dt02335a.

CCDC 2490597–2490599 contain the supplementary crystallographic data for this paper.[21a–c]

Acknowledgements

The authors thank the National Institute of Science Education and Research (NISER), Homi Bhabha National Institute (HBNI), Bhubaneswar, and the Department of Atomic Energy (DAE), Govt. of India. The Science and Engineering Research Board (SERB), India (CRG/2021/007000) is acknowledged for providing financial support.

References

1 (*a*) A. Baishya, M. K. Barman, T. Peddarao and S. Nembenna, *J. Organomet. Chem.*, 2014, **769**, 112–118; (*b*) D. K. Nayak, N. Sarkar, C. M. Sampath, R. K. Sahoo and S. Nembenna, *Z. Anorg. Allg. Chem.*, 2022, **648**, e202200116; (*c*) T. G. Ong, J. S. O'Brien, I. Korobkov and D. S. Richeson, *Organometallics*, 2006, **25**, 4728–4730; (*d*) R. K. Sahoo, A. G. Patro, N. Sarkar and S. Nembenna, *Organometallics*, 2023, **42**, 1746–1758; (*e*) S. Dagorne, I. A. Guzei, M. P. Coles and R. F. Jordan, *J. Am. Chem. Soc.*, 2000, **122**, 274–289; (*f*) G. J. Durant, *Chem. Soc. Rev.*, 1985, **14**, 375–398; (*g*) D. M. Makley and J. N. Johnston, *Org. Lett.*, 2014, **16**, 3146–3149; (*h*) I. Ojima and S.-i. Inaba, *J. Organomet. Chem.*, 1977, **140**, 97–111; (*i*) V. Verma, A. Koperniku, P. M. Edwards and L. L. Schafer, *Chem. Commun.*, 2022, **58**, 9174–9189; (*j*) T. Ishikawa, *Chem. Pharm. Bull.*, 2010, **58**, 1555–1564; (*k*) C. Alonso-Moreno, A. Antiñolo, F. Carrillo-Hermosilla and A. Otero, *Chem. Soc. Rev.*, 2014, **43**, 3406–3425; (*l*) N. Kaur, M. Rajput and P. Bhardwaj, *Synth. Commun.*, 2022, **52**, 1547–1580.

2 E. W. Thomas, E. E. Nishizawa, D. C. Zimmermann and D. J. Williams, *J. Med. Chem.*, 1989, **32**, 228–236.

3 A. Baishya, T. Peddarao, M. K. Barman and S. Nembenna, *New J. Chem.*, 2015, **39**, 7503–7510.

4 P. K. Vardhanapu, V. Bheemireddy, M. Bhunia, G. Vijaykumar and S. K. Mandal, *Organometallics*, 2018, **37**, 2602–2608.

5 T. G. Ong, G. P. A. Yap and D. S. Richeson, *J. Am. Chem. Soc.*, 2003, **125**, 8100–8101.

6 (*a*) J. Bhattacharjee, A. Harinath, I. Banerjee, H. P. Nayek and T. K. Panda, *Inorg. Chem.*, 2018, **57**, 12610–12623; (*b*) H. Shen, H.-S. Chan and Z. Xie, *Organometallics*, 2006, **25**, 5515–5517; (*c*) F. Montilla, A. Pastor and A. Galindo, *J. Organomet. Chem.*, 2004, **689**, 993–996.

7 (*a*) R. J. Batrice and M. S. Eisen, *Chem. Sci.*, 2016, **7**, 939–944; (*b*) Z. Du, W. Li, X. Zhu, F. Xu and Q. Shen, *J. Org. Chem.*, 2008, **73**, 8966–8972; (*c*) B. Jing, C. Zhu, F. Wang, J. Li and C. Cui, *Organometallics*, 2024, **43**, 2314–2320; (*d*) I. S. R. Karmel, M. Tamm and M. S. Eisen, *Angew. Chem., Int. Ed.*, 2015, **54**, 12422–12425; (*e*) Q. Li, S. Wang, S. Zhou, G. Yang, X. Zhu and Y. Liu, *J. Org. Chem.*, 2007, **72**, 6763–6767; (*f*) H. Liu, N. Fridman, M. Tamm and M. S. Eisen, *Organometallics*, 2017, **36**, 3896–3903; (*g*) S. Zhou, S. Wang, G. Yang, Q. Li, L. Zhang, Z. Yao, Z. Zhou and H.-b. Song, *Organometallics*, 2007, **26**, 3755–3761.

8 (*a*) W. X. Zhang, L. Xu and Z. Xi, *Chem. Commun.*, 2015, **51**, 254–265; (*b*) J. R. Lachs, A. G. M. Barrett, M. R. Crimmin, G. Kociok-Köhn, M. S. Hill, M. F. Mahon and P. A. Procopiou, *Eur. J. Inorg. Chem.*, 2008, **2008**, 4173–4179; (*c*) C. N. Rowley, T. G. Ong, J. Priem, T. K. Woo and D. S. Richeson, *Inorg. Chem.*, 2008, **47**, 9660–9668; (*d*) W.-X. Zhang, D. Li, Z. Wang and Z. Xi, *Organometallics*, 2009, **28**, 882–887; (*e*) C. Alonso-Moreno, F. Carrillo-Hermosilla, A. Garcés, A. Otero, I. López-Solera, A. M. Rodríguez and A. Antiñolo, *Organometallics*, 2010, **29**, 2789–2795; (*f*) J. Koller and R. G. Bergman, *Organometallics*, 2010, **29**, 5946–5952.

9 (*a*) F. B. Dains and E. W. Brown, *J. Am. Chem. Soc.*, 1909, **31**, 1148–1157; (*b*) I. Orchard, G. J. P. Singh and B. G. Loughton, *Comp. Biochem. Physiol., C*, 1982, **73**, 331–334; (*c*) N. Miyaura and A. Suzuki, *Chem. Rev.*, 1995, **95**, 2457–2483; (*d*) K. S. Hayes, *Appl. Catal., A*, 2001, **221**, 187–195; (*e*) J. S. Carey, D. Laffan, C. Thomson and M. T. Williams, *Org. Biomol. Chem.*, 2006, **4**, 2337–2347; (*f*) M. Pelckmans, T. Renders, S. Van de Vyver and B. F. Sels, *Green Chem.*, 2017, **19**, 5303–5331.

10 (*a*) W. Ma, L. Xu, W.-X. Zhang and Z. Xi, *New J. Chem.*, 2015, **39**, 7649–7655; (*b*) C. D. Huke and D. L. Kays, in *Advances in Organometallic Chemistry*, ed. P. J. Pérez, Academic Press, 2021, vol. 75, pp. 1–54; (*c*) A. R. Bazkiaei, M. Findlater and A. E. V. Gorden, *Org. Biomol. Chem.*, 2022, **20**, 3675–3702; (*d*) K. Bano, J. Sharma, A. Jain, H. Tsurugi and T. K. Panda, *RSC Adv.*, 2023, **13**, 3020–3032.

11 (*a*) S. Rajput, R. K. Sahoo, N. M. T. and S. Nembenna, *Chem. Commun.*, 2024, **60**, 11148–11151; (*b*) S. Mukhopadhyay, A. Das, S. Padhan and S. Nembenna, *Inorg. Chim. Acta*, 2026, **589**, 122924.

12 (*a*) A. Das, S. Rej and T. K. Panda, *Dalton Trans.*, 2022, **51**, 3027–3040; (*b*) J. E. Seok, H. T. Kim, J. Kim, J. H. Lee, A. K. Jaladi, H. Hwang and D. K. An, *Asian J. Org. Chem.*, 2022, **11**, e202200405; (*c*) T. Chu and G. I. Nikonov, *Chem. Rev.*, 2018, **118**, 3608–3680; (*d*) C. Weetman and S. Inoue, *ChemCatChem*, 2018, **10**, 4213–4228; (*e*) R. L. Melen, *Science*, 2019, **363**, 479–484; (*f*) S. Inoue, R. L. Melen and S. Harder, *Eur. J. Inorg. Chem.*, 2022, **2022**, e202200414.

13 (*a*) M. Arrowsmith, T. J. Hadlington, M. S. Hill and G. Kociok-Köhn, *Chem. Commun.*, 2012, **48**, 4567–4569; (*b*) M. Arrowsmith, M. S. Hill and G. Kociok-Köhn, *Chem. – Eur. J.*, 2013, **19**, 2776–2783; (*c*) C. Weetman, M. D. Anker, M. Arrowsmith, M. S. Hill, G. Kociok-Köhn, D. J. Liptrot and M. F. Mahon, *Chem. Sci.*, 2016, **7**, 628–641; (*d*) C. Weetman, M. S. Hill and M. F. Mahon, *Chem. – Eur. J.*, 2016, **22**, 7158–7162; (*e*) M. Magre, B. Maity, A. Falconnet, L. Cavallo and M. Rueping, *Angew. Chem., Int. Ed.*, 2019, **58**, 7025–7029; (*f*) D. Elorriaga, F. Carrillo-Hermosilla, A. Antiñolo, I. López-Solera, R. Fernández-Galán, A. Serrano and E. Villaseñor, *Eur. J. Inorg. Chem.*, 2013, **2013**, 2940–2946; (*g*) M. De Tullio, A. Hernán-Gómez, Z. Livingstone, W. Clegg, A. R. Kennedy, R. W. Harrington, A. Antiñolo, A. Martínez, F. Carrillo-Hermosilla and E. Hevia, *Chem. – Eur. J.*, 2016, **22**, 17646–17656; (*h*) D. Mukherjee and J. Okuda, *Angew. Chem., Int. Ed.*, 2018, **57**, 1458–1473; (*i*) M. M. Roy, A. A. Omana, A. S. Wilson, M. S. Hill, S. Aldridge and E. Rivard, *Chem. Rev.*, 2021, **121**, 12784–12965; (*j*) R. Kumar, S. Dutta, V. Sharma, P. P. Singh, R. G. Gonnade, D. Koley and S. S. Sen, *Chem. – Eur. J.*, 2022, **28**, e202201896; (*k*) H. J. Han, H. T. Kim, J. Kim, A. K. Jaladi and D. K. An, *Tetrahedron*, 2023, **142**, 133500; (*l*) J. Shi, M. Luo, X. Zhang, T. Yuan, X. Chen and M. Ma, *Org. Biomol. Chem.*, 2023, **21**, 3628–3635; (*m*) C. Ginés, B. Parra-Cadenas, R. Fernández-Galán, D. García-Vivó, D. Elorriaga, A. Ramos and F. Carrillo-Hermosilla, *Adv. Synth. Catal.*, 2025, **367**, e202400843; (*n*) B. Mahata, V. Devaraj, S. R. Dash, R. G. Gonnade, K. Vanka and S. S. Sen, *Inorg. Chem.*, 2025, **64**, 13405–13414; (*o*) S. Yadav, R. Dixit, M. K. Bisai, K. Vanka and S. S. Sen, *Organometallics*, 2018, **37**, 4576–4584; (*p*) R. Kumar, V. Sharma, S. Banerjee, K. Vanka and S. S. Sen, *Chem. Commun.*, 2023, **59**, 2255–2258; (*q*) R. Kumar, B. Mahata, S. Gayathridevi, K. Vipin Raj, K. Vanka and S. S. Sen, *Chem. – Eur. J.*, 2024, **30**, e202303478.

14 (*a*) C. Bakewell, *Dalton Trans.*, 2020, **49**, 11354–11360; (*b*) M. Magre, M. Szewczyk and M. Rueping, *Curr. Opin. Green Sustainable Chem.*, 2021, **32**, 100526; (*c*) J. R. Lynch, A. R. Kennedy, J. Barker, J. Reid and R. E. Mulvey, *Helv. Chim. Acta*, 2022, **105**, e202200082; (*d*) D. Parveen, S. Saha, R. Kumar Yadav, S. K. Pati and D. Kumar Roy, *Chem. – Asian J.*, 2025, **20**, e202401853; (*e*) S. Ramkumar, S. Reddappa, S. Mohan, K. Pramoda and S. K. Bose, *ChemCatChem*, 2025, **17**, e00206.

15 R. Lalrempuia, C. E. Kefalidis, S. J. Bonyhady, B. Schwarze, L. Maron, A. Stasch and C. Jones, *J. Am. Chem. Soc.*, 2015, **137**, 8944–8947.

16 A. G. M. Barrett, I. J. Casely, M. R. Crimmin, M. S. Hill, J. R. Lachs, M. F. Mahon and P. A. Procopiou, *Inorg. Chem.*, 2009, **48**, 4445–4453.

17 (*a*) J. Zhang, R. Cai, L. Weng and X. Zhou, *Organometallics*, 2004, **23**, 3303–3308; (*b*) W. X. Zhang, M. Nishiura and Z. Hou, *Synlett*, 2006, 1213–1216; (*c*) W. X. Zhang, M. Nishiura and Z. Hou, *Chem. – Eur. J.*, 2007, **13**, 4037–4051.

18 (*a*) A. D. Bage, T. A. Hunt and S. P. Thomas, *Org. Lett.*, 2020, **22**, 4107–4112; (*b*) A. D. Bage, K. Nicholson, T. A. Hunt, T. Langer and S. P. Thomas, *ACS Catal.*, 2020, **10**, 13479–13486; (*c*) J. Macleod and S. P. Thomas, *Nat. Chem.*, 2025, DOI: 10.1038/s41557-025-01955-0.

19 P. J. Bailey, R. A. Coxall, C. M. Dick, S. Fabre, L. C. Henderson, C. Herber, S. T. Liddle, D. Loroño-González, A. Parkin and S. Parsons, *Chem. – Eur. J.*, 2003, **9**, 4820–4828.

20 G. R. Fulmer, A. J. M. Miller, N. H. Sherden, H. E. Gottlieb, A. Nudelman, B. M. Stoltz, J. E. Bercaw and K. I. Goldberg, *Organometallics*, 2010, **29**, 2176–2179.

21 (*a*) CCDC 2490597: Experimental Crystal Structure Determination, 2025, DOI: 10.5517/ccdc.csd.cc2plnvt; (*b*) CCDC 2490598: Experimental Crystal Structure Determination, 2025, DOI: 10.5517/ccdc.csd.cc2plnwv; (*c*) CCDC 2490599: Experimental Crystal Structure Determination, 2025, DOI: 10.5517/ccdc.csd.cc2plnxw.